PETROLOGY OF METAMORPHIC ROCKS IN THE OSWALDGRABEN (GLEINALM AREA, EASTERN ALPS, STYRIA)

by

Sara Raič, Aberra Mogessie, Kurt Krenn & Georg Hoinkes

Institut für Erdwissenschaften
Universität Graz, Universitätsplatz 2, A-8010 Graz, Österreich

Abstract

The investigated area in the Oswaldgraben contains a sequence of metamorphic rocks of garnet-micaschists, amphibolites, paragneisses and marbles. It is located in the Gleinalm area directly at the transition to the Graz Paleozoic. The study shows that this sequence is of Eoalpine monometamorphic character and can be explained as the eastern continuation of the monometamorphic units of the Radenthein Complex. This is based on a detailed petrographic and electron microprobe study of mineral phases identified in the different rock types. Metapelitic garnets have a composition in the range of $Alm_{57-74} Prp_{6-14} Grs_{9-21} Sps_{1-4}$ and garnets from metabasites (garnet-amphibolites) range around $Alm_{60-73} Prp_{12-23} Grs_{5-20} Sps_{1-4}$. Amphiboles in the garnet-amphibolites are calcic-amphiboles and correspond mainly to tschermakitic hornblendes and tschermakites. Analyzed feldspars (in garnet-micaschists, garnet-amphibolites) have a composition ranging from oligoclase (An_{11-29}) - andesine (An_{31-36}) to minor albite (An_{10}), with an exception of the feldspars in the marbles that are mainly orthoclase. Biotites can be classified as phlogopite, meroxene and lepidomelane. Garnet-biotite-thermometry and garnet-amphibole-plagioclase-barometry on garnet-amphibolites results in pressure- and temperature conditions of around 10 kbar and 660°C.

Geological Overview

The evolution of the Eoalpine orogen (i.e. Cretaceous orogeny) started with the still ongoing convergence between the African and European plates in the Upper Jurassic about 150 Ma ago. Due to the convergent movements parts of the rocks of the Eastern Alps experienced a high P/T gradient ("Eo-Alpine High Pressure Belt", THÖNI 1981; Fig. 1). Remaining units are considered as upper plate units (e.g. Ötztal-Bundschuh Nappe System and Paleozoic nappe systems; Fig. 1), which have been overthrusted by the highest nappe units, the Northern Calcareous Alps (Upper Austroalpine). Today the whole units of the Eastern Alps are dominated by eastward extrusion accompanied by the formation of large-scale shear zones and extensional normal faults.
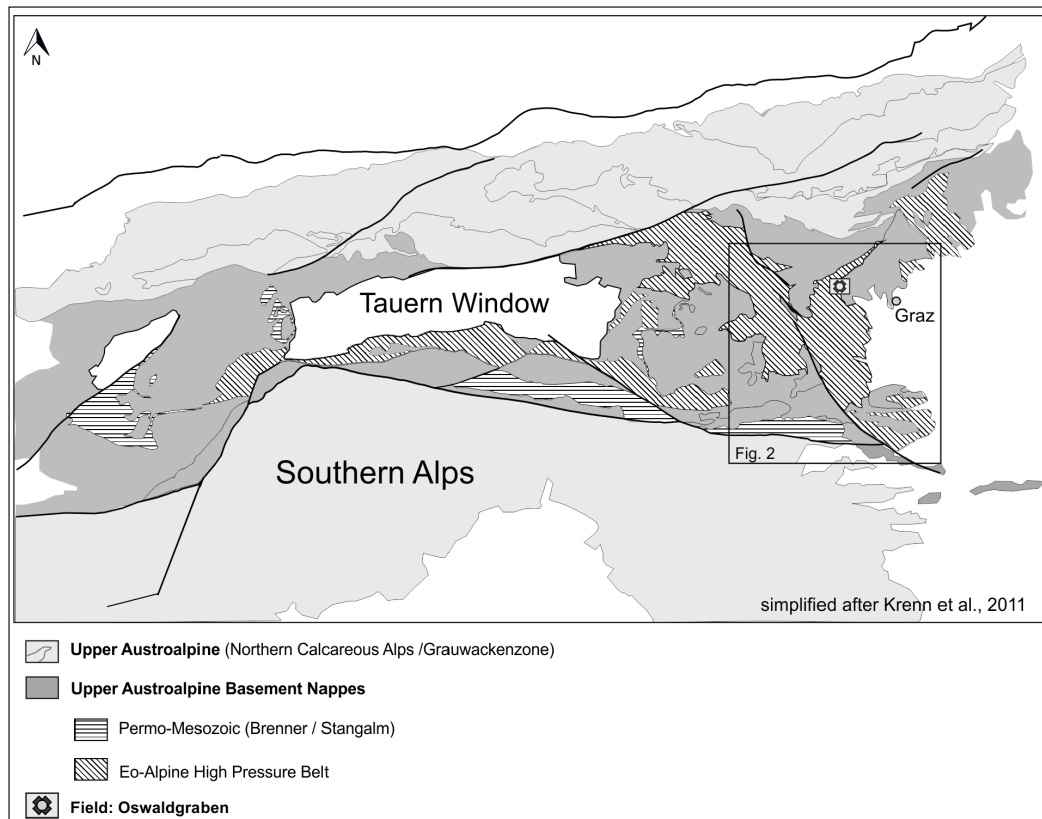
Fig .1

Geological map showing the tectonic units of the Eastern Alps with the project area indicated as rectangle.

The geology of Styria consists of the Upper Austroalpine including the Paleozoic Grauwackenzone, the Upper Austroalpine basement nappes and parts of the Lower Austroalpine nappes (for detailed information see SCHMID et al. 2004).

The study area in the "Oswaldgraben" is located near the transition between the Graz Paleozoic as part of the Drauzug-Gurktal nappe system in the south and the Koralpe-Wölz nappe system as part of the "Eo-Alpine High Pressure Belt". Beside the Eoalpine event the lithologies of the Koralpe-Wölz nappe system are characterized by a polymetamorphic evolution showing remnants of two Prealpine events (Variscan and Permian) which are mainly preserved in garnets of metapelites as relics. However, metapelites exist which have experienced only one metamorphism, the so-called "monometamorphic units", which can probably be considered as the eastern continuation of the Radenthein Complex (Fig. 1). In this study, representative samples were collected for detailed petrographic and petrological study in order to find out if the rocks from this region belong to a polymetamorphic unit (i.e. Rappold Complex) or to a probable eastern continuation of the monometamorphic units (Fig. 2).

The Rappold Complex and the monometamorphic units differ in their metamorphic imprint, which is mainly reflected by mineral assemblages of garnet-micaschists containing poly- and monometamorphic garnet generations, respectively.
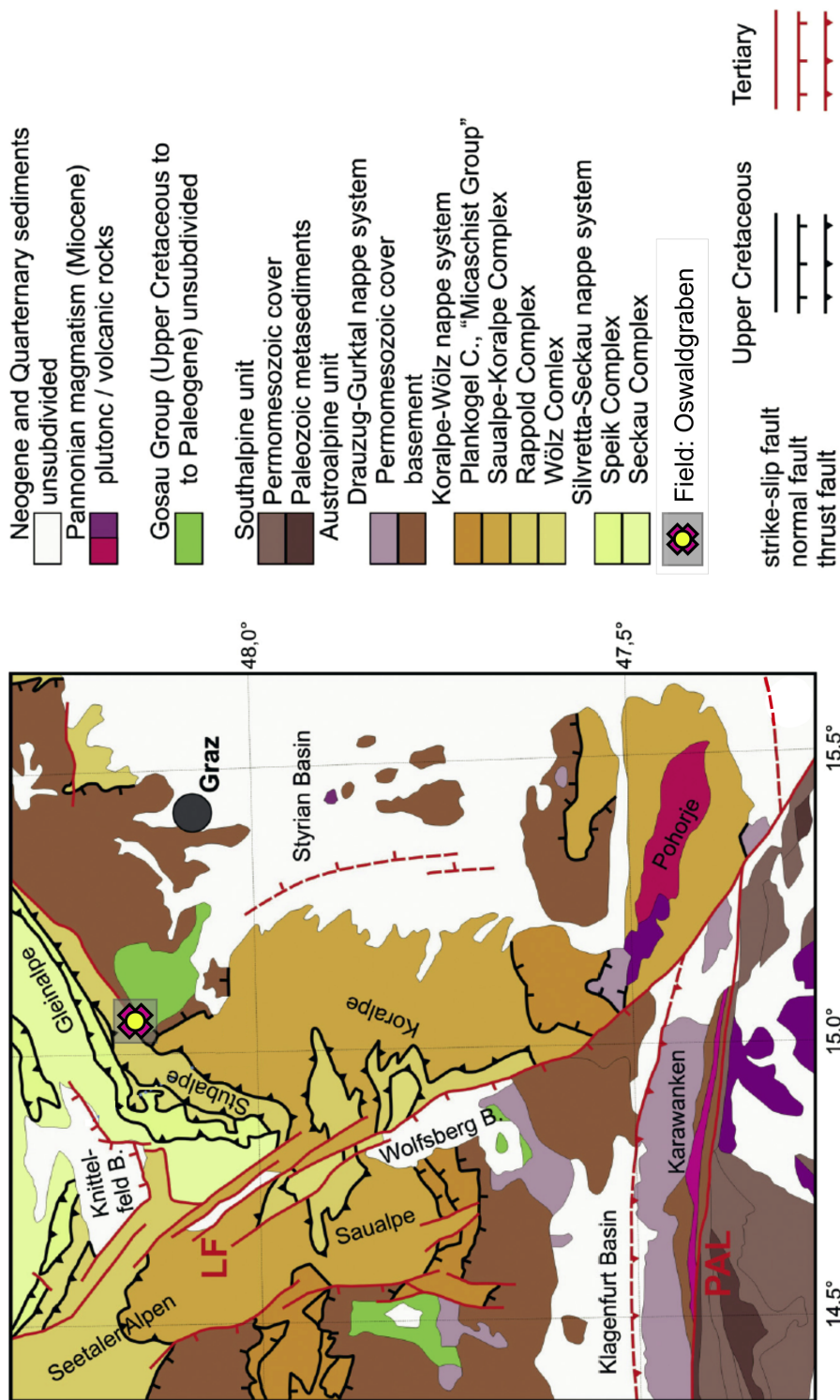
Neogene and Quarternary sediments
unsubdivided

Pannonian magmatism (Miocene)
plutonc / volcanic rocks

Gosau Group (Upper Cretaceous to
to Paleogene) unsubdivided

Southalpine unit
Permomesozoic cover
Paleozoic metasediments

Austroalpine unit
Drauzug-Gurktal nappe system
Permomesozoic cover
basement

Koralpe-Wölz nappe system
Plankogel C., "Micaschist Group"
Saualpe-Koralpe Complex
Rappold Complex
Wölz Comlex

Silvretta-Seckau nappe system
Speik Complex
Seckau Complex

Field: Oswaldgraben

strike-slip fault
normal fault
thrust fault

Upper Cretaceous

Tertiary

48,0°

47,5°

Graz
Styrian Basin

Gleinalpe
Knittel-
feld B.
Seetaler Alpen
LF
Saualpe
Wolfsberg B.
Stubalpe
Koralpe
Pohorje
Karawanken
Klagenfurt Basin
PAL

14,5°   15,0°   15,5°

Fig. 2
Tectonic map of the Austroalpine units in the Gleinalpe, Koralpe and Saualpe area (HOINKES et al., 2010).

69

Hence, garnets belonging to the Rappold Complex should reflect a major element zonation which shows a clear "jump" in their Ca-content whereas garnets belonging to the monometamorphic units are characterized by a continuous zonation pattern. The Rappold Complex itself is dominated by paragneisses, micaschists and minor amphibolites.

Petrography of lithologies in the Oswaldgraben

Garnet-micaschist

The mineral assemblages of the micaschists are very similar and differ basically in the modal abundance of the different phases documented in the samples. This leads to the following nomenclature: garnet-micaschist, graphite-bearing biotite-garnet-micaschist and garnet-hornblende-micaschist. In general, these rocks contain quartz, plagioclase, large garnet grains several mm in-size, biotite, chlorite, muscovite, clinozoisite, epidote and accessories. The garnet grains are mostly coated with graphite at the rims leading to a slight optical zoning of garnets. Garnets contain inclusions of quartz, plagioclase, elongated clinozoisite, epidote, zircon, tourmaline and opaque phases. All these phases can also occur in cracks in garnet.
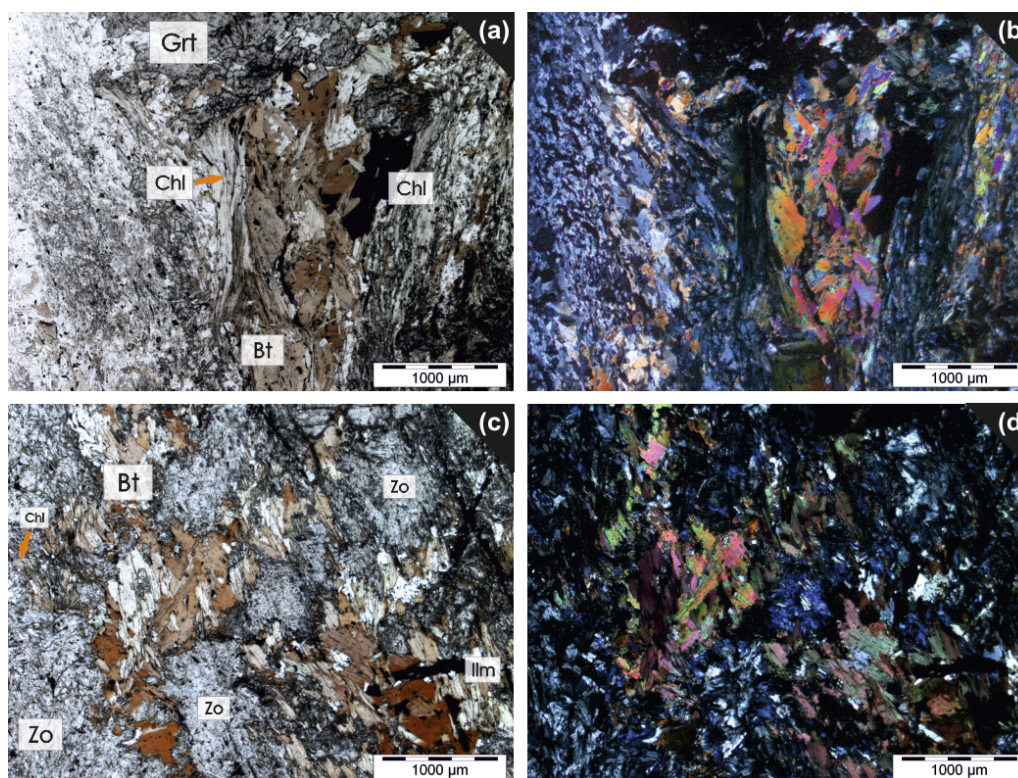

Fig. 3(a-d)

Photomicrographs of garnet-micaschists (a) Sample RO1 with Grt, Chl and Bt (b) sample RO1 with crossed nicols (c) sample RO4 with Bt, Chl and Czo, showing the frequent concentration of needle-like clinozoisites as small agglomerations distributed over the entire matrix (d) sample RO4 with crossed nicols.

In some micaschists garnet grains are retrogressed and replaced by chlorite, biotite and plagioclase at the rim (Figs. 3a and b). Additionally rims can be overgrown by opaque phases or amphiboles of a short-prismatic habitus. Amphiboles are ferro-tschermakites and contain several inclusions of zoisite, epidote, chlorite, rutile and zircon. Biotite is also partly replaced by chlorite (Figs. 3a and b) and encloses minerals like zircon and opaque phases. Chlorite shows a partly radial growth with varying grain size and sometimes anomalous blue interference colors between crossed polarizers. Accumulations of different matrix minerals like clinozoisite and epidote without any preferred orientation are observed (Figs. 3c and d). The clinozoisites, however, develop fine-grained needle-like variably oriented crystals, which can form accumulations, but also spread throughout the whole sample. Quartz- and plagioclase layers crosscut by elongated clinozoisite grains and sericitic alterations of plagioclase are also present. Quartz shows a partly undulous extinction as well as a "core-mantle-texture", caused by the growth of new recrystallized grains around larger former quartz cores.

Garnet-amphibolite

The metabasites mainly consist of mm-sized amphiboles and garnet besides chlorite, biotite, epidote, quartz, plagioclase and sericite. Accessories are tourmaline, apatite and opaque phases. Garnet is partly fragmented and contains inclusions of quartz, plagioclase, chlorite, epidote and opaque phases.
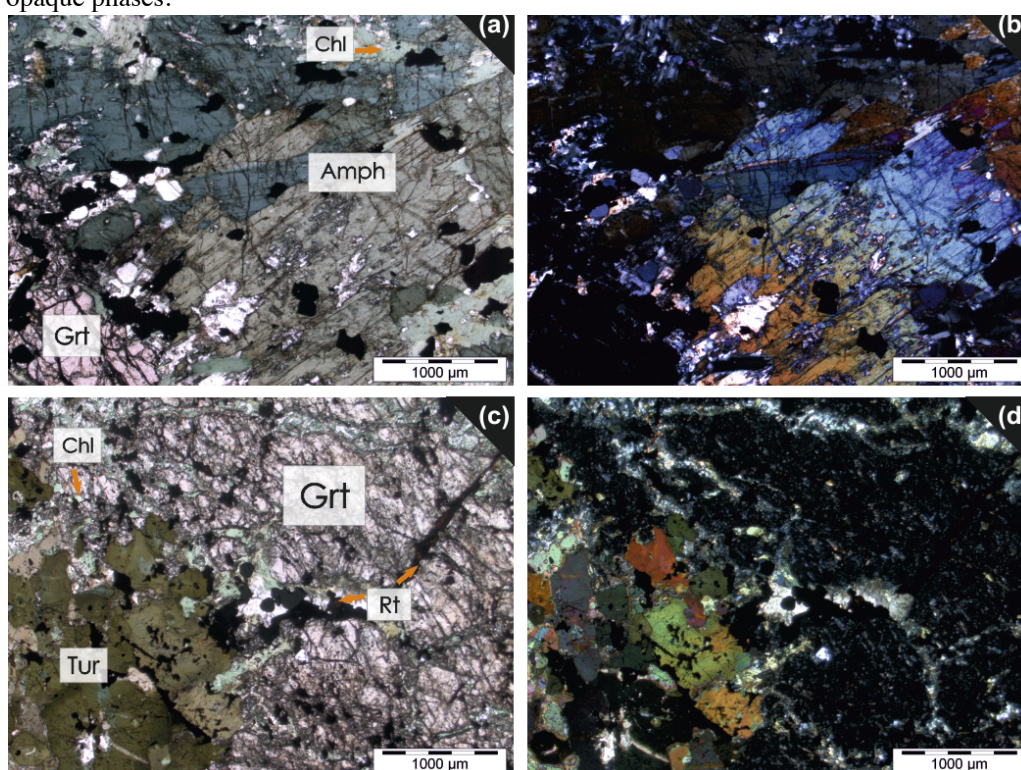

Fig. 4 (a-d)
Photomicrographs of garnet amphibolites (a) sample RO17 with Amph, Grt and Chl (b) sample RO17 with crossed nicols (c) sample RO12 with Grt, Chl, Tur and Rt, showing the large turmalines (d) sample RO12 with crossed nicols.

These inclusions can be very fine- to coarse-grained. Garnet can be replaced at the rim by biotite and chlorite. Chlorite occurs in the matrix, grows partly in garnet cracks or replaces the primary biotite. The shape of the amphiboles is almost acicular and locally short-prismatic (Figs. 4a and b). Smaller, differently orientated amphiboles grow at the grain boundaries of some large amphiboles. Sericitic alteration is observed in plagioclase enclosed in amphibole. Amphibole rims are often replaced by radial growing chlorite. Large, zoned and inclusion-rich tourmalines (Figs. 4c and d) with grain size in mm range overgrow garnets or occur together with amphiboles. They contain inclusions of plagioclase, quartz, epidote and numerous opaque phases, like rutile, ilmenite and pyrite.

Paragneisses
The studied gneisses show a major variation in the modal abundance of their minerals, grain size and deformation mechanisms. Hence the following different types of gneisses have been identified and investigated:
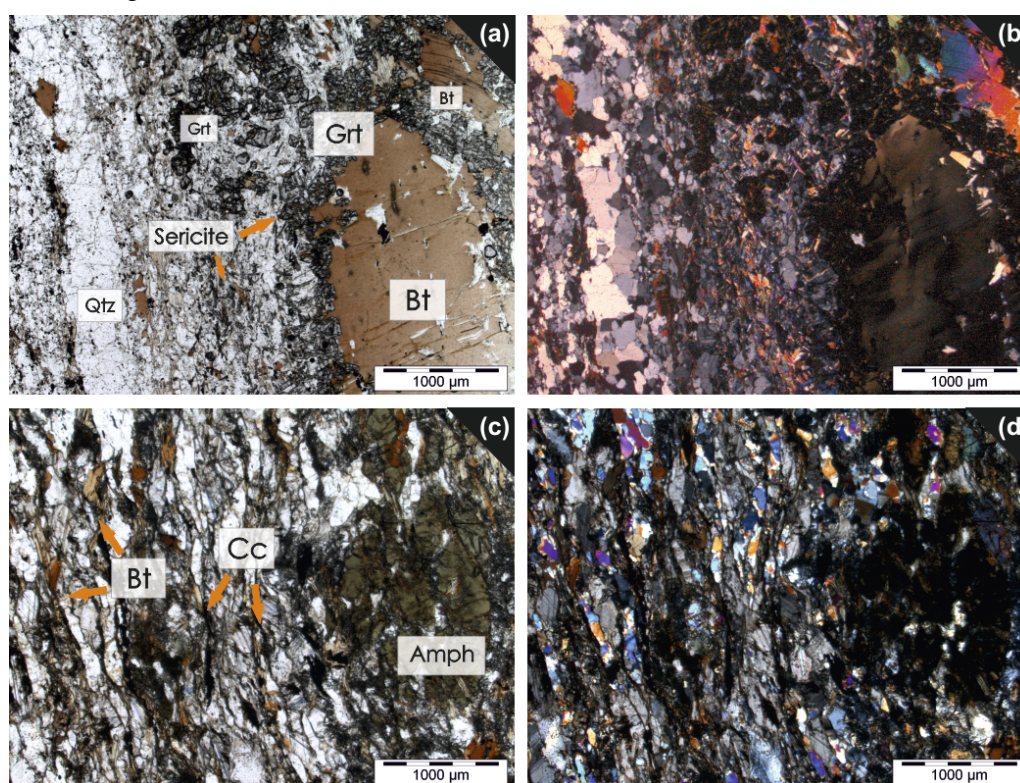

Fig. 5 (a-d)
Photomicrographs of different paragneisses (a) sample RO5 with Grt, Bt, sericite and Qtz (b) sample RO5 with crossed nicols (c) sample RO6 with Amph, Bt and Cc (d) sample RO6 with crossed nicols.

1. Garnet-biotite-plagioclase-gneiss: mainly consist of garnet, quartz, plagioclase, biotite, muscovite, clinozoisite, epidote and accessory opaque phases. The garnets are fragmented, full of cracks and contain inclusions of biotite, quartz, occasionally epidote and opaque phases.

Garnets typically occur as mm-sized crystals associated with large biotite grains (Figs. 5a and b). Plagioclase appears sericitic. Sometimes accumulations of small, elongated clinozoisites with anomalous blue interference colors, overgrowing the matrix minerals, occur.

2. Hornblende-garnet-biotite-plagioclase gneiss: contains porphyroblasts of hornblende, garnet, and accessories of rutile and ilmenite in a fine-grained matrix of quartz, plagioclase, biotite, zoisite and carbonate (Figs. 5c and d).

3. Biotite-plagioclase gneiss with the paragenesis plagioclase + quartz + biotite + muscovite + chlorite + carbonate + zoisite + epidote + accessories is strongly deformed but without any preferred orientation of the mineral phases. Accumulations of zoisite, quartz, carbonate and epidote can be found in the whole sample. Fine-grained biotite- and muscovite needles are partly overgrowing the carbonate minerals.

Marble

Marble consists of calcite and occasionally phlogopite platelets. Feldspar occurs rarely. Opaque phases like graphite, pyrite, coated by oxides, pyrrhotite and chalcopyrite occur as accessory phases with different grain sizes.
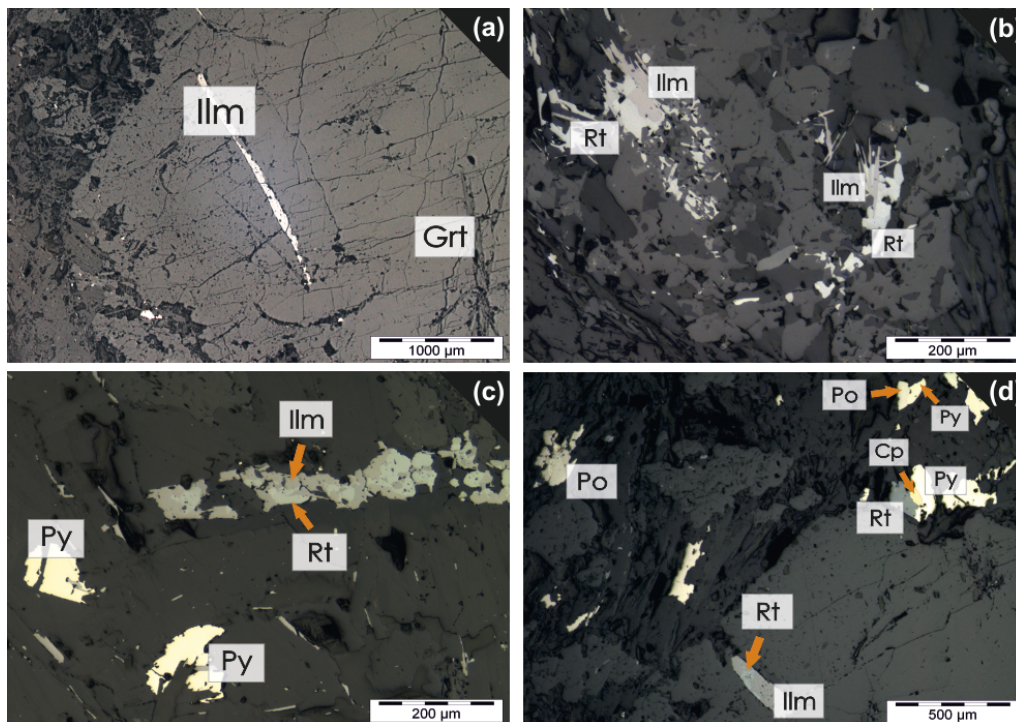

Fig. 6 (a-d)

Photomicrographs using reflected light microscopy (a) sample RO1 with Ilm in Grt (b) sample RO6 with Ilm-Rt-segragtions (c) sample RO4 with Ilm-Rt-segreagtion and Py (d) sample RO1 with paragenesis of oxides and sulfides.

73

Opaque phases

Rutile, ilmenite and segregations of these two mineral phases occur in the matrix, and also over-grow amphiboles, garnets and other matrix minerals (Fig. 6a and b). In addition magnetite, pyrite, pyrrhotite and chalcopyrite are also documented. Assemblages of ilmenite, magnetite and pyrrhotite are common, as well as oxides rimming pyrrhotite grains (Fig. 6c and d). Small graphite grains with brownish color and undulous extinction are found in all the investigated samples, mainly in marbles.

Mineral chemistry

Garnet

In general all garnets are relatively almandine-rich and have composition Alm_{57-74} Prp_{6-14} Grs_{9-21} Sps_{1-4} (Tab. 1). Garnets from metabasites (garnet-amphibolites) have composition Alm_{60-73} Prp_{12-23} Grs_{5-20} Sps_{1-4}.

Mineral	Garnet							
Rock	Garnet-micaschist				Garnet-amphibolite			
Sample	RO1	RO3	RO4	RO4	RO10	RO12	RO17	RO17
SiO_2	37.74	37.67	37.78	37.83	38.46	37.74	38.25	37.82
TiO_2	0.00	0.10	0.10	0.02	0.08	0.00	0.00	0.07
Al_2O_3	20.48	20.46	20.52	20.39	21.54	20.58	20.75	20.48
Fe_2O_3	0.00	0.00	0.00	0.70	0.12	0.23	0.28	0.80
FeO	29.90	29.04	31.33	28.94	28.13	28.59	29.64	29.16
MnO	2.10	3.34	1.55	0.67	0.93	0.52	2.22	1.90
MgO	1.56	1.51	1.76	3.12	4.76	3.63	5.11	5.04
CaO	7.91	7.60	7.21	7.86	6.65	7.44	3.71	4.07
Na_2O	0.00	0.00	0.00	0.00	0.00	0.00	0.00	0.00
K_2O	0.00	0.00	0.00	0.00	0.00	0.00	0.00	0.00
Total	99.69	99.77	100.24	99.53	100.67	98.73	99.99	99.34
Normalization on the basis of 12 oxygens								
Si	3.04	3.03	3.03	3.02	3.00	3.02	3.02	3.01
Ti	0.00	0.01	0.01	0.00	0.00	0.00	0.00	0.00
Al	1.94	1.94	1.94	1.92	1.98	1.94	1.93	1.92
Fe^{3+}	0.00	0.00	0.00	0.04	0.01	0.01	0.02	0.05
Fe^{2+}	2.01	1.95	2.10	1.93	1.84	1.91	1.96	1.94
Mn	0.14	0.23	0.11	0.05	0.06	0.04	0.15	0.13
Mg	0.19	0.18	0.21	0.37	0.55	0.43	0.60	0.60
Ca	0.68	0.66	0.62	0.67	0.56	0.64	0.31	0.35
Na	0.00	0.00	0.00	0.00	0.00	0.00	0.00	0.00
K	0.00	0.00	0.00	0.00	0.00	0.00	0.00	0.00
Σ Cations	8.00	8.00	8.00	8.00	8.00	8.00	8.00	8.00
Endmembers								
Alm	0.67	0.65	0.69	0.64	0.61	0.63	0.65	0.64
Prp	0.06	0.06	0.07	0.12	0.18	0.14	0.20	0.20
Sps	0.05	0.08	0.04	0.02	0.02	0.01	0.05	0.04
Grs	0.23	0.21	0.20	0.20	0.18	0.20	0.09	0.09
$X_{Mg}(Fe^{2+})$	0.09	0.09	0.09	0.16	0.23	0.19	0.24	0.24

Table 1

Representative electron microprobe analyses of garnet in metapelites and metabasites.
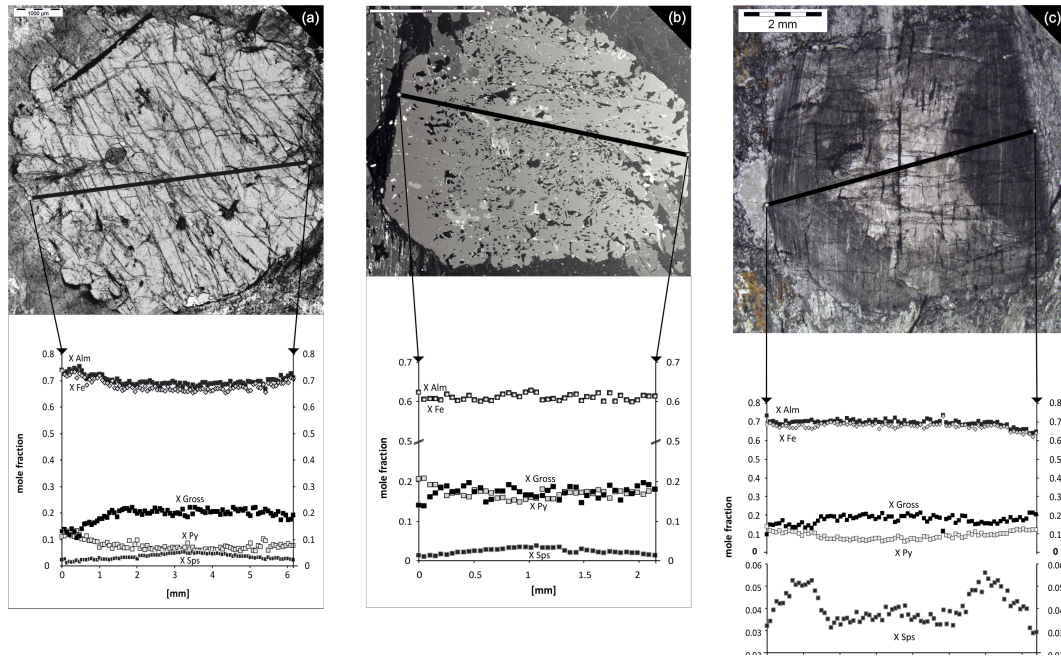
Fig. 7 (a-c)
garnet profiles (a) sample RO1 (b) sample RO10 (c) sample RO4.

Major element zoning shows a general trend in composition where Mg and Fe increase and Ca and Mn decrease towards the rims (Fig. 7).

Sample RO1 contains inclusion-free garnets and sample RO10 inclusion-rich garnets (Fig. 7a and b). Garnet grains show a bell-shaped curve for X_{Sps} in the core (Fig. 7a and b). Both types of garnets reflect a continuous zonation and suggest a prograde character with a slight decrease in pressure. In sample RO4 the X_{Sps} has lower values in the core and becomes higher towards the rim and finally decreases at the outer rim (Fig. 7c). This trend can be correlated with the inclusion patterns in the studied garnet, where the rim shows a clear internal foliation contrasting to the core.

Amphibole

Amphiboles in the garnet-amphibolites are calcic-amphiboles (Tab. 2) and correspond mainly to tschermakitic hornblendes and tschermakites with $X_{Mg} = 0.52 - 0.681$, $(Na+K)_A = 0.34 - 0.48$ and $(Ca+Na)_B = 1.76 - 1.89$. Ca_B lies between 1.41 and 1.62 and Na_B between 0.23 and 0.42. $Al^{(IV)}$ varies in tschermaktic hornblendes between 1.632 and 1.75 and in tschermakites between 1.751 and 1.875 (Figs. 8a and b). Depending on their coexisting minerals, amphiboles show a different cation distribution. Amphiboles coexisting with garnet (almandine) are Fe-rich at the rims. Amphiboles coexisting with feldspar (albite) show a decrease in Ca and Al, and an increase in Na. Except sample RO1 (ferro-tschermakites), all measured amphiboles can be described as tschermakitic hornblendes or tschermakites.
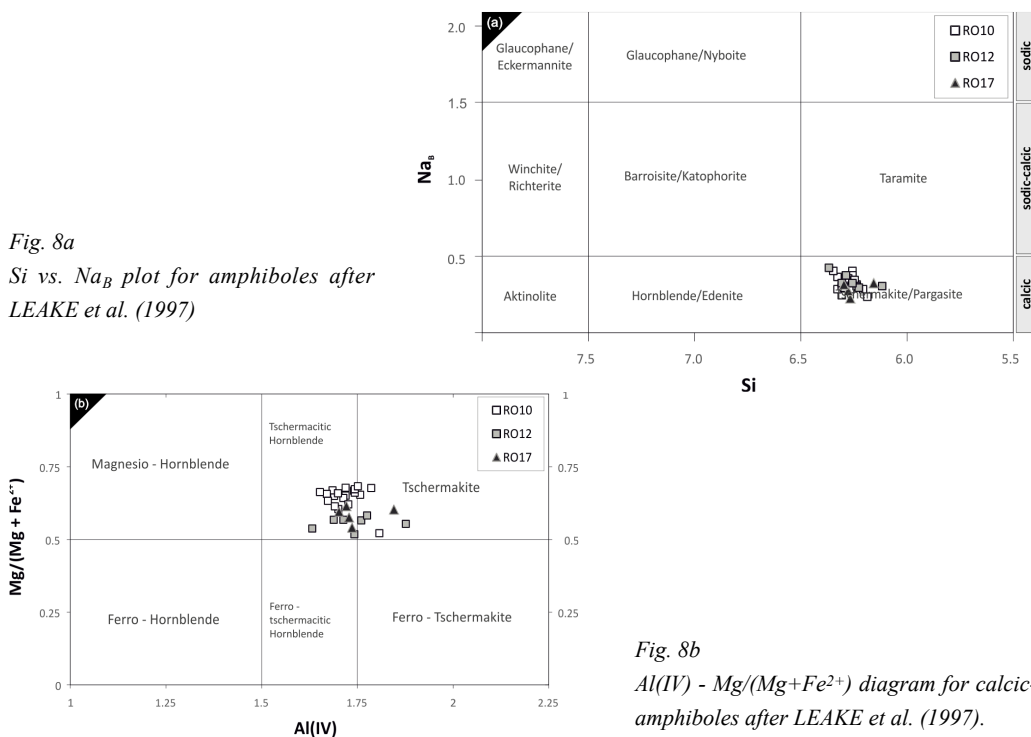
Mineral	Amphibole*					Biotite				
Rock	Garnet-amphibolite							Garnet-micaschist		
Sample	RO10	RO10	RO12	RO17	RO17	RO17	RO17	RO1	RO3	RO4
SiO₂	41.74	42.81	42.01	42.98	43.32	38.35	35.99	37.44	36.13	36.43
TiO₂	0.31	0.53	0.60	0.53	0.40	1.47	1.04	1.46	2.47	1.62
Al₂O₃	16.55	16.36	15.66	15.64	15.68	17.29	16.02	18.70	18.63	17.95
Fe₂O₃	4.72	4.86	4.98	3.48	4.39	0.00	0.00	0.00	0.00	0.00
FeO	13.47	10.01	12.03	12.42	11.70	14.77	16.83	17.61	19.88	17.67
MnO	0.16	0.00	0.00	0.12	0.15	0.00	0.13	0.09	0.13	0.01
MgO	8.18	10.50	8.82	9.64	10.02	14.91	13.58	11.88	9.05	11.66
CaO	10.18	9.86	9.16	10.07	9.84	0.00	0.07	0.00	0.00	0.00
Na₂O	1.84	2.19	2.11	2.61	2.65	0.19	0.13	0.18	0.18	0.10
K₂O	0.32	0.25	0.47	0.28	0.25	8.85	8.18	7.74	9.42	9.38
Total	97.47	97.37	95.84	97.77	98.40	95.83	91.97	95.10	95.89	94.82
	Normalization on basis of 23 oxygens					*Normalization on basis of 11 oxygens*				
Si	6.19	6.24	6.29	6.30	6.30	2.84	2.80	2.81	2.80	2.80
Ti	0.03	0.06	0.07	0.06	0.04	0.08	0.06	0.08	0.14	0.09
Al$^{(IV)}$	1.81	1.76	1.71	1.70	1.70	1.16	1.20	1.19	1.20	1.20
Al$^{(VI)}$	1.09	1.06	1.05	1.01	0.99	0.35	0.26	0.47	0.51	0.43
Fe^{3+}	0.53	0.53	0.56	0.38	0.48	0.00	0.00	0.00	0.00	0.00
Fe^{2+}	1.67	1.22	1.51	1.52	1.42	0.92	1.09	1.11	1.29	1.14
Mn	0.02	0.00	0.00	0.01	0.02	0.00	0.01	0.01	0.01	0.00
Mg	1.81	2.28	1.97	2.11	2.17	1.65	1.57	1.33	1.05	1.34
Ca	1.62	1.54	1.47	1.58	1.53	0.00	0.01	0.00	0.00	0.00
Na	0.53	0.62	0.61	0.74	0.75	0.03	0.02	0.03	0.03	0.01
K	0.06	0.05	0.09	0.05	0.05	0.84	0.81	0.74	0.93	0.92
Σ Cations	15.36	15.36	15.32	15.47	15.46	7.86	7.84	7.77	7.95	7.93
X$_{Mg}$(Fe^{2+})	0.52	0.65	0.57	0.58	0.60	0.64	0.59	0.55	0.45	0.54

* Sample RO10 = Tschermakites; samples RO12 and RO17 = tschermakitic hornblendes

Table 2

Representative electron microprobe analyses of amphibole and biotite in metapelites and metabasites.
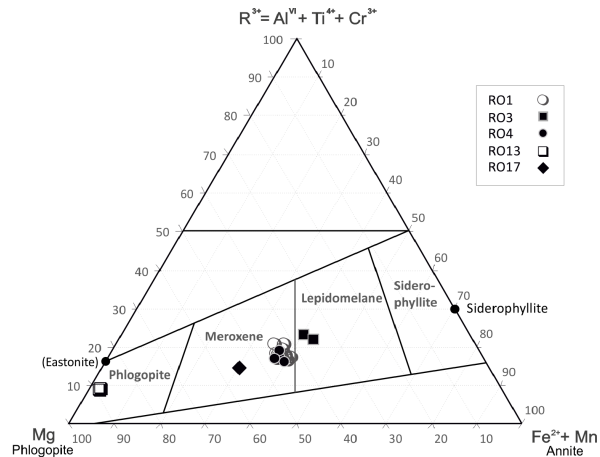

Fig. 8a

Si vs. Na$_B$ plot for amphiboles after LEAKE et al. (1997)

Fig. 8b

Al(IV) - Mg/(Mg+Fe^{2+}) diagram for calcic-amphiboles after LEAKE et al. (1997).

Biotite

Based on $Mg - (Fe^{2+} + Mn) - R^{3+}$ ($R^{3+} = Al^{(VI)} + Ti^{4+} + Cr^{3+}$) the biotites can be classified as phlogopite (in marble), meroxene and lepidomelane (in garnet-mica-schists and garnet-amphibolites; Fig. 10). Analyzed biotites show FeO contents ranging between 16 and 20 wt. % and MgO contents between 9 and 13 wt. % (Tab. 2). Al_2O_3 has average value of 18 wt. %.

Fig. 10

Classification of measured biotites based on the plot $Mg - (Fe^{2+} + Mn) - R^{3+}$ ($R^{3+} = Al^{IV} + Ti^{4+} + Cr^{3+}$).

Feldspar

All analyzed feldspars (in garnet-micaschists, garnet-amphibolites) have a composition ranging from oligoclase (An_{11-29}) - andesine (An_{31-36}) to minor albite (An10). Feldspars in marbles are mainly orthoclase in character (Tab. 3 and Fig. 9).

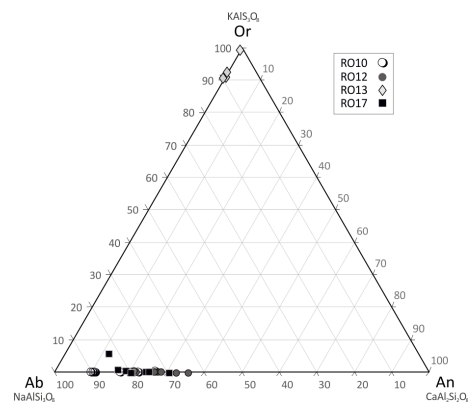| Mineral	Plagioclase				
Rock	Garnet-amphibolite				
Sample	RO10	RO10	RO12	RO17	RO17
SiO₂	66.21	66.34	62.62	65.40	63.87
TiO₂	0.00	0.00	0.00	0.00	0.02
Al₂O₃	21.38	21.72	23.67	22.69	22.79
Fe₂O₃	0.00	0	0.00	0.00	0.00
FeO	0.16	0.11	0.08	0.09	0.12
MnO	0.13	0.05	0.00	0.03	0.01
MgO	0.00	0	0.18	0.00	0.07
CaO	2.16	2.06	5.36	2.34	4.44
Na₂O	9.98	10.07	8.56	9.18	9.01
K₂O	0.06	0.07	0.03	0.98	0.06
Total	100.08	100.42	100.51	100.69	100.39
Normalization on the basis of 8 oxygens					
Si	2.92	2.91	2.76	2.87	2.82
Ti	0.00	0.00	0.00	0.00	0.00
Al	1.11	1.12	1.23	1.18	1.19
Fe³⁺	0.00	0.00	0.00	0.00	0.00
Fe²⁺	0.01	0.00	0.00	0.00	0.00
Mn	0.00	0.00	0.00	0.00	0.00
Mg	0.00	0.00	0.01	0.00	0.00
Ca	0.10	0.10	0.25	0.11	0.21
Na	0.85	0.86	0.73	0.78	0.77
K	0.00	0.00	0.00	0.05	0.00
∑ Cations	5.00	5.00	5.00	4.99	4.99
Endmembers					
An	0.11	0.101	0.26	0.12	0.21
Ab	0.89	0.895	0.74	0.83	0.78
Or	0.00	0.004	0.00	0.06	0.00

Fig. 9

Projection of feldspar chemical data into the ternary Or-Ab-An-system.

Table 3

Representative electron microprobe analyses of plagioclase.

Chlorite

The FeO content in chlorites varies between 17 and 32 wt. %, the MnO contents however range between 0.05 and 0.18 wt. %. Chlorites, coexisting with garnets have FeO-values between 26 and 32 wt. %. The MgO-values range between 12 and 15 wt. %, which may be explained by the Fe-Mg-exchange between garnet and chlorite. The FeO-values of chlorites coexisting with micas and feldspars range between 21 and 24 wt. %; the MgO-content ranges between 16 and 18 wt. % and the Al_2O_3-content lies between 22 and 24 wt. %. Chlorite crystals adjacent to amphiboles display significantly lower FeO-values compared to other minerals which are in contact with chlorite. FeO content reaches 17 wt. % and their MgO-contents between 20 and 22 wt. %.

Epidote and clinozoisite

Analyzed epidotes have a CaO composition reaching 23 wt. % and Al2O3 values between 25 and 27 wt. % (Fig. 11 and Tab. 4). The Fe_2O_3 content lies between 8 and 10.5 wt. % and shows clearly higher values compared to clinozoisites which reach up to 6 wt. %. Clinozoisites in contrast have CaO compositions ranging between 22 and 25 wt. % and Al_2O_3 values between 29 and 32 wt. %. The pistacite component is ranging between 5 and 21 mol%.

Mineral	Epidote-group minerals					
Rock	Garnet-micaschist				Garnet-amphibolite	
Sample	RO1	RO1	RO3	RO4	RO12	RO12
SiO₂	38.89	38.91	39.77	39.49	37.50	38.20
TiO₂	0.05	0.00	0.00	0.00	0.02	0.13
Al₂O₃	28.80	29.38	30.96	30.10	24.84	26.62
Cr₂O₃	0.00	0.07	0.01	0.00	0.09	0.00
Fe₂O₃	5.88	5.37	2.68	4.49	10.54	8.00
FeO	0.00	0.00	0.00	0.00	0.00	0.00
MnO	0.14	0.06	0.03	0.11	0.02	0.03
MgO	0.00	0.26	0.03	0.08	0.27	0.21
CaO	23.99	24.12	24.45	24.49	22.01	22.50
Na₂O	0.00	0.00	0.00	0.00	0.27	0.21
K₂O	0.01	0.00	0.11	0.00	0.00	0.00
Total	97.76	98.17	98.04	98.76	95.56	95.90
Normalization on the basis of 12 oxygens and 1 OH-group						
Si	3.01	3.00	3.04	3.01	3.02	3.04
Ti	0.00	0.00	0.00	0.00	0.00	0.01
Al	2.63	2.67	2.79	2.71	2.36	2.50
Cr	0.00	0.00	0.00	0.00	0.01	0.00
Fe³⁺	0.34	0.31	0.15	0.26	0.64	0.48
Fe²⁺	0.00	0.00	0.00	0.00	0.00	0.00
Mn	0.01	0.00	0.00	0.01	0.00	0.00
Mg	0.00	0.03	0.00	0.01	0.03	0.03
Ca	1.99	1.99	2.00	2.00	1.90	1.92
Na	0.00	0.00	0.00	0.00	0.00	0.00
K	0.00	0.00	0.01	0.00	0.00	0.00
Σ Cations	7.99	8.01	8.00	8.00	7.97	7.97

Table 3

Representative electron microprobe analyses of epidote-group minerals.
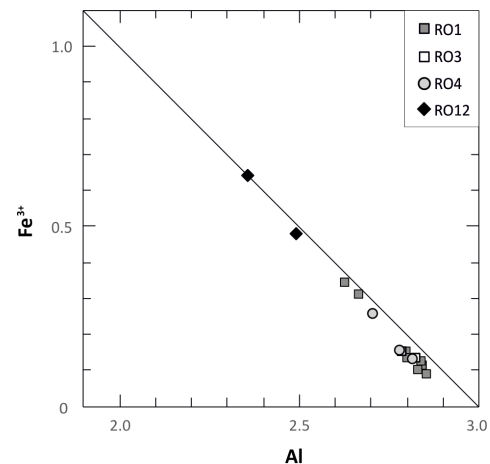

Fig. 11

Al vs. Fe^{3+} diagram for epidote-group minerals.

Geothermobarometry

The garnet-amphibole-plagioclase-barometer (after DALE et al., 2000) was applied for pressure calculations. Garnet-biotite- and garnet-chlorite-thermometry were used for temperature calculation according to the calibrations of HOLDAWAY (2000) and PERCHUK (1991), respectively. Based on garnet-biotite-thermometry, garnet-amphibolites (samples RO10, RO12 and RO17) give the following pressure-temperature conditions: Sample RO10 yields pressures between 10.5 to 11.2 kbar and temperatures in the range of 690 - 710° (Fig. 12a). Garnet-Chlorite-thermometry was used for sample RO12 and results in T 610 - 640°C. Pressure conditions range around 6.8 - 9.8 kbar (Fig. 12b). For sample RO17 garnet-biotite-thermometry and garnet-chlorite-thermometry give temperatures between 650 - 680°C and 610 - 640°C, respectively. Pressure conditions are around 5.8 - 9.8 kbar (Fig. 12c).
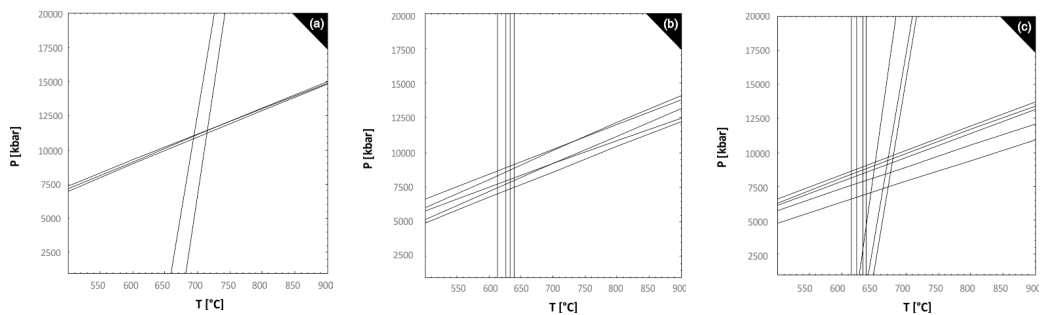

Fig. 12 (a-c)

(a) Garnet-biotite-thermometry (HOLDAWAY, 2000) and garnet-amphibole-plagioclase-barometry (DALE et al., 2000) for sample RO10 (b) Garnet-chlorite-thermometry (PERCHUK, 1991) and garnet-amphibole-plagioclase-barometry (DALE et al., 2000) for sample RO12 (c) Garnet-biotite- (HOLDAWAY, 2000) and garnet-chlorite-thermometry (PERCHUK, 1991) and garnet-amphibole-plagioclase-barometry (DALE et al., 2000) for sample RO17.

Conclusion

This study which deals with a lithological sequence of metamorphic rocks (garnet-micaschist, garnet-amphibolite and marble) in the Oswaldgraben shows that directly at the transition to the Graz Paleozoic a unit consisting of lithologies with monometamorphic character is exposed. Compared to the monometamorphic units further west, i.e. the Radenthein Complex, an eastern continuation of Eoalpine monometamorphic rocks in the Gleinalm area can be expected that needs further investigations about its regional extent. The analyzed garnets show a chemical zonation that is comparable to the garnets with monometamorphic character further west (SCHUSTER & FRANK, 1999; SCHUSTER et al. 2004), which can be described as continuous growth during one single metamorphic event. Almandine is the dominant garnet endmember. Amphiboles are calcic-amphiboles that correspond mainly to tschermakitic hornblendes, tschermakites and ferro-tschermakites. P-T estimates are comparable to conditions from monometamorphic sequences of the Eoalpine high-pressure wedge further west (HOINKES et al. 1999) and support its existence in the southern Gleinalm area.

References

ARMBRUSTER, T., BONAZZI, P., AKASAKA, M., BERMANEC, V., CHOPIN, C., GIERÉ, R., HEUSS-ASSBICHLER, S., LIEBSCHER, A., MENCHETTI, S., PAN Y., PASERO, M. (2006): Recommended nomenclature of epidote-group minerals. European Journal of Mineralogy, vol.18, 551-567.

BAILEY, S. W. (1988): Chlorites: Structures and crystal chemistry: in BAILEY, S. W., editor, Hydrous Phyllo-silicates (exclusive of micas), v. 19 in Reviews in Mineralogy, Mineralogical Society of America, Washington, D. C, 347-403.

BECKER, L. P. (1980): Geologische Karte der Republik Österreich 1:50000, Erläuterungen zu Blatt 162 Köflach. Geologische Bundesanstalt, Wien.

BEST, M. G. (2003): Igneous and metamorphic petrology. 2nd edition, Blackwell Publishing, 1-729

DALE J., HOLLAND T., POWELL R. (2000): Hornblende-garnet-plagioclase thermobarometry: a natural assemblage calibration of the thermodynamics of hornblende. Contrib. Miner. Petrol., 140, 353-362

DACHS E. (1998): PET: Petrological elementary tools for Mathematica. Computers & Geosciences 24/3, 219-235.

FAYRAD, S. W. & HOINKES, G. (2003): P-T gradient of EO-Alpine metamorphism within the Austroalpine base-ment units east of the Tauern Window (Austria). Mineralogy and Petrology, 77, 129-159.

HEY, M. H. (1954): A new review of chlorites. – Min. Mag., 30, 278-292.

HOINKES, G., KOLLER, F., DEMÉNY, A., SCHUSTER, R., MILLER, C., THÖNI, M., KURZ, W., KRENN, K., WALTER, F. (2010): Metamorphism in the Eastern Alps. ACTA Mineralogica-Petrographica, Field Guide Series, vol. 1, 1-47.

HOLDAWAY, J. (2000): Application of new experimental and garnet Magules data to the garnet-biotite geot-hermometer. American Mineralogist, vol.85, no.7-8, 881-892.

KRENN K., KURZ W., FRITZ H., HOINKES G. (2011): Eoalpine tectonics of the Eastern Alps: implications from the evolution of monometamprphic Austroalpine units (Schneeberg and Radenthein Complex). Swiss Journal of Geosciences, 104, 471-491.

KURZ, W. & FRITZ, H. (2003): Tectonometamorphic evolution of the Austroalpine nappe complex in the central Eastern Alps – Consequences for the Eo-Alpine Evolution of the Eastern Alps. International Geological Review, vol. 45, no. 12, 1100-1127.

LEAKE, B. E. (1978): Nomenclature of amphiboles. The Canadian Mineralogist., vol. 16, 501-520.

LEAKE B. E., WOOLLEY A. R., ARPS C. E. S., GILBERT M. C., GRICE J. D., HAWTHORNE F. C., KATIO A., KISCH H. J., KRIVOVICHEV V. G., LINTHOUT K., LAIRD J., MANDARINO J. A., MARESCH W. V., NICKEL E. H., ROCK N. M. S., SCHUHMACHER J. C., SMITH D. C., STEPHENSON N. C. N., UNGARETTI L., WHITTAKER E. J. W., YOUCHZI G. (1997): Nomenclature of Amphiboles: Report of the subcommittee on amphiboles of the international mineralogical association, commission on new minerals and mineral names. The Canadian Mineralogist, vol. 35, 219-246.

MOGESSIE, A., ETTINGER., K., LEAKE, B. E. (2004): Nomenclature of amphiboles: Additions and revisions to the International Mineralogical Association's amphibole nomenclature. Mineralogical Magazine, vol. 68, 209-215.

NEUBAUER, F., DALLMEYER, R. D., DUNKL, I., SCHIRNIK, D. (1995): Late Cretaceous exhumation of the metamorphic Gleinalm dome, Eastern Alps" kinematics, cooling history and sedimentary response in a sinistral wrench corridor. Tectonophysics, 242, 79-98.

NEUBAUER, F. (1988): Bau und Entwicklungsgeschichte des Rennfeld-Mugel- und des Gleinalm-Kristallins (Ostalpen). Abhandlungen der geologischen Bundesanstalt. Band 42, 1-137.

OELSNER, O. (1961): Atlas der wichtigsten Mineralparagenesen im mikroskopischen Bild. 1. Auflage, VEB, Deutscher Verlag der Wissenschaften, Berlin, 1-309.

OKRUSCH, M. & MATTHES, S. (2009): Mineralogie, Eine Einführung in die spezielle Mineralogie, Petrologie und Lagerstättenkunde, 8. Auflage, Springer, Berlin Heidelberg, 1-658.

PERCHUK, L. L. (1991): Progress in Metamorphic and Magmatic Petrology: A Memorial Volume in Honor of D.S. Korzinsky. Cambridge Univ. Press, London, 93-111.

SCHIRNIK, D. (1994): Sedimentologie, Palöopedogenese und Geröllanalyse in der Kainacher Gosau. - Unveröff.Diss. Universität Graz, 1-305.

SCHMID, S. M., FÜGENSCHUH, B., KISSLING, E. & SCHUSTER, R. (2004): Tectonic map and overall architecture of the Alpine orogen. Eclogae Geologicae Helvetiae, 97, 93–117.

SCHUSTER, R., BERNHARD, F., HOINKES, G., KAINDL, R., KOLLER, F., LEBER, T., MELCHER, F., PUHL, J. (1999): Exkursion to the Eastern Alps. Metamorphism at the eastern end of the Alps – Alpine, Permo-Triassic, Variscan?. Mitteilungen der Deutschen Mineralogischen Gesellschaft, Beiheft zum European Journal of Mineralogy, 11, Beih. 2, pereprint.

SCHUSTER, R., KOLLER, F., HOECK, V., HOINKES, G., BOUSQUET, R. (2004): Explenatory notes to the map: metamorphic structure of the alps, metamorphic evolution of the eastern alps. Mitt. Österr. Miner. Ges. 149.

SCHUSTER, R., PESTAL, G. & REINER, J. M. (2006): Geologische Karte der Republik Österreich 1:50000, Erläuterungen zu Blatt 182 Spittal an der Drau. Geologische Bundesanstalt, Wien.

SPEAR, F. S. (1993): Metamorphic Phase Equilibria and Pressure-Temperature-Time-Paths, Mineralogical Society of America, Monograph, Washington D. C., 1-799.

SPEAR, F.S. & KIMBALL, K.L. (1984): Recamp – A Fortran IV program for estimating Fe^{3+} contents in amphiboles. Computers in Geology, 10, 317-325.

THÖNI, M. (1981): Degree and evolution of the Alpine Metamorphism in the Austroalpine Unit W of the Tauern Window in light of K/Ar and Rb/S rage determinations on Micas. Jahrbuch der Geologischen Bundesanstalt, 124, 111-174.

TOLLMANN, A. (1977): Geologie von Österreich, Band 1, Die Zentralalpen. p.1-766. Deuticke, Wien.

TRÖGER, W.E. (1971): Optische Bestimmung der gesteinsbildenden Minerale. Teil 1: Bestimmungstabellen. Schweizerbart, Stuttgart, 1-188.